

A New Angle on Gravitational Clustering

Román Scoccimarro

*Institute for Advanced Study, School of Natural Sciences,
Einstein Drive, Princeton, NJ 08540*

Abstract. We describe a new approach to gravitational instability in large-scale structure, where the equations of motion are written and solved as in field theory in terms of Feynman diagrams. The basic objects of interest are the propagator (which propagates solutions forward in time), the vertex (which describes non-linear interactions between waves) and a source with prescribed statistics which describes the effect of initial conditions. We show that loop corrections renormalize these quantities, and discuss applications of this formalism to a better understanding of gravitational instability and to improving non-linear perturbation theory in the transition to the non-linear regime. We also consider the role of vorticity creation due to shell-crossing and show using N-body simulations that at small (virialized) scales the velocity field reaches equipartition, i.e. the vorticity power spectrum is about twice the divergence power spectrum.

1. Standard Formulation of Gravitational Instability

Assuming the initial velocity field is irrotational, gravitational instability can be described completely in terms of the density field and the velocity divergence, $\theta \equiv \nabla \cdot \mathbf{v}$. Defining the conformal time $\tau = \int dt/a$ and the conformal expansion rate $\mathcal{H} \equiv d \ln a / d\tau$, the equations of motion in Fourier space become

$$\frac{\partial \tilde{\delta}(\mathbf{k})}{\partial \tau} + \tilde{\theta}(\mathbf{k}) = - \int d^3 k_1 d^3 k_2 [\delta_D] \alpha(\mathbf{k}, \mathbf{k}_1) \tilde{\theta}(\mathbf{k}_1) \tilde{\delta}(\mathbf{k}_2), \quad (1)$$

$$\frac{\partial \tilde{\theta}(\mathbf{k})}{\partial \tau} + \mathcal{H} \tilde{\theta}(\mathbf{k}) + \frac{3}{2} \Omega \mathcal{H}^2 \tilde{\delta}(\mathbf{k}) = - \int d^3 k_1 d^3 k_2 [\delta_D] \beta(\mathbf{k}_1, \mathbf{k}_2) \tilde{\theta}(\mathbf{k}_1) \tilde{\theta}(\mathbf{k}_2), \quad (2)$$

where $[\delta_D] = \delta_D(\mathbf{k} - \mathbf{k}_{12})$, \mathbf{k} is a comoving wave number, and

$$\alpha(\mathbf{k}, \mathbf{k}_1) \equiv \frac{\mathbf{k} \cdot \mathbf{k}_1}{k_1^2}, \quad \beta(\mathbf{k}_1, \mathbf{k}_2) \equiv \frac{k^2(\mathbf{k}_1 \cdot \mathbf{k}_2)}{2k_1^2 k_2^2}. \quad (3)$$

Equations (1) and (2) are valid in an arbitrary homogeneous and isotropic universe, which evolves according to the Friedmann equations:

$$\frac{\partial \mathcal{H}(\tau)}{\partial \tau} = -\frac{\Omega}{2} \mathcal{H}^2(\tau) + \frac{\Lambda}{3} a^2(\tau), \quad (4)$$

$$(\Omega - 1)\mathcal{H}^2(\tau) = k - \frac{\Lambda}{3}a^2(\tau), \quad (5)$$

where Λ is the cosmological constant, the spatial curvature constant $k = -1, 0, 1$ for $\Omega_{\text{tot}} < 1$, $\Omega_{\text{tot}} = 1$, and $\Omega_{\text{tot}} > 1$, respectively, and $\Omega_{\text{tot}} \equiv \Omega + \Omega_\Lambda$, with $\Omega_\Lambda \equiv \Lambda a^2 / (3\mathcal{H}^2)$. For $\Omega = 1$, the perturbative growing mode solutions are given by

$$\tilde{\delta}(\mathbf{k}) = \sum_{n=1}^{\infty} a^n(\tau) \delta_n(\mathbf{k}), \quad (6)$$

$$\tilde{\theta}(\mathbf{k}) = \mathcal{H}(\tau) \sum_{n=1}^{\infty} a^n(\tau) \theta_n(\mathbf{k}). \quad (7)$$

Modelling the matter as pressureless non-relativistic ‘dust’, an appropriate description for cold dark matter before shell crossing, the fluid equations of motion determine $\delta_n(\mathbf{k})$ and $\theta_n(\mathbf{k})$ in terms of the linear fluctuations,

$$\delta_n(\mathbf{k}) = \int d^3q_1 \dots \int d^3q_n [\delta_{\text{D}}]_n F_n^{(s)}(\mathbf{q}_1, \dots, \mathbf{q}_n) \delta_1(\mathbf{q}_1) \dots \delta_1(\mathbf{q}_n), \quad (8)$$

$$\theta_n(\mathbf{k}) = - \int d^3q_1 \dots \int d^3q_n [\delta_{\text{D}}]_n G_n^{(s)}(\mathbf{q}_1, \dots, \mathbf{q}_n) \delta_1(\mathbf{q}_1) \dots \delta_1(\mathbf{q}_n), \quad (9)$$

where $[\delta_{\text{D}}]_n \equiv \delta_{\text{D}}(\mathbf{k} - \mathbf{q}_1 - \dots - \mathbf{q}_n)$. The functions $F_n^{(s)}$ and $G_n^{(s)}$ are constructed from the mode coupling functions $\alpha(\mathbf{k}, \mathbf{k}_1)$ and $\beta(\mathbf{k}_1, \mathbf{k}_2)$ by a recursive procedure (Goroff et al. 1986),

$$F_n(\mathbf{q}_1, \dots, \mathbf{q}_n) = \sum_{m=1}^{n-1} \frac{G_m(\mathbf{q}_1, \dots, \mathbf{q}_m)}{(2n+3)(n-1)} \left[(2n+1)\alpha(\mathbf{k}, \mathbf{k}_1) F_{n-m}(\mathbf{q}_{m+1}, \dots, \mathbf{q}_n) + 2\beta(\mathbf{k}_1, \mathbf{k}_2) G_{n-m}(\mathbf{q}_{m+1}, \dots, \mathbf{q}_n) \right], \quad (10)$$

$$G_n(\mathbf{q}_1, \dots, \mathbf{q}_n) = \sum_{m=1}^{n-1} \frac{G_m(\mathbf{q}_1, \dots, \mathbf{q}_m)}{(2n+3)(n-1)} \left[3\alpha(\mathbf{k}, \mathbf{k}_1) F_{n-m}(\mathbf{q}_{m+1}, \dots, \mathbf{q}_n) + 2n\beta(\mathbf{k}_1, \mathbf{k}_2) G_{n-m}(\mathbf{q}_{m+1}, \dots, \mathbf{q}_n) \right] \quad (11)$$

(where $\mathbf{k}_1 \equiv \mathbf{q}_1 + \dots + \mathbf{q}_m$, $\mathbf{k}_2 \equiv \mathbf{q}_{m+1} + \dots + \mathbf{q}_n$, $\mathbf{k} \equiv \mathbf{k}_1 + \mathbf{k}_2$, and $F_1 = G_1 \equiv 1$). In Eqs.(8-9), $F_n^{(s)}$ and $G_n^{(s)}$ are the symmetrized version of F_n and G_n , respectively.

From these perturbative solutions a number of important results have been derived in the literature, most of them regarding the tree-level (leading-order) behavior of correlation functions, e.g. Fry (1984), Goroff et al. (1986), Bernardeau (1992,1994). Loop calculations have been attempted only in some particular cases (Scoccimarro & Frieman 1996; Scoccimarro 1997, Scoccimarro et al. 1998); although in the spherical collapse approximation a number of useful results have been obtained (Fosalba & Gaztañaga 1998; Gaztañaga & Fosalba 1998).

2. Field Theory Approach

2.1. Integral Form of the Equations of Motion

The equations of motion can be rewritten in a more symmetric form by defining a two-component “vector” $\Psi_a(\mathbf{k}, z)$, where $a = 1, 2$, $z \equiv \ln a$, and:

$$\Psi_a(\mathbf{k}, z) \equiv \begin{pmatrix} \delta(\mathbf{k}, z), & -\theta(\mathbf{k}, z)/\mathcal{H} \end{pmatrix}, \quad (12)$$

which for $\Omega = 1$ leads to the following equations of motion (we henceforth use the convention that repeated Fourier arguments are integrated over)

$$\partial_z \Psi_a(\mathbf{k}, z) + \Omega_{ab} \Psi_b(\mathbf{k}, z) = \gamma_{abc}(\mathbf{k}, \mathbf{k}_1, \mathbf{k}_2) \Psi_b(\mathbf{k}_1, z) \Psi_c(\mathbf{k}_2, z), \quad (13)$$

where

$$\Omega_{ab} \equiv \begin{bmatrix} 0 & -1 \\ -3/2 & 1/2 \end{bmatrix}, \quad (14)$$

and γ_{abc} is a matrix given by

$$\gamma_{121}(\mathbf{k}, \mathbf{k}_1, \mathbf{k}_2) = \delta_{\text{D}}(\mathbf{k} - \mathbf{k}_{12}) \alpha(\mathbf{k}, \mathbf{k}_1), \quad (15)$$

$$\gamma_{222}(\mathbf{k}, \mathbf{k}_1, \mathbf{k}_2) = \delta_{\text{D}}(\mathbf{k} - \mathbf{k}_{12}) \beta(\mathbf{k}_1, \mathbf{k}_2), \quad (16)$$

and zero otherwise. The somewhat complicated expressions for the PT kernels recursion relations in the previous section can be easily derived in this formalism. The perturbative solutions read

$$\Psi_a(\mathbf{k}, z) = \sum_{n=1}^{\infty} e^{nz} \psi_a^{(n)}(\mathbf{k}), \quad (17)$$

which leads to

$$(n\delta_{ab} + \Omega_{ab}) \psi_b^{(n)}(\mathbf{k}) = \gamma_{abc}(\mathbf{k}, \mathbf{k}_1, \mathbf{k}_2) \sum_{m=1}^{n-1} \psi_b^{(n-m)}(\mathbf{k}_1) \psi_c^{(m)}(\mathbf{k}_2). \quad (18)$$

Now, let $\sigma_{ab}^{-1}(n) \equiv n\delta_{ab} + \Omega_{ab}$, then we have:

$$\psi_a^{(n)}(\mathbf{k}) = \sigma_{ab}(n) \gamma_{bcd}(\mathbf{k}, \mathbf{k}_1, \mathbf{k}_2) \sum_{m=1}^{n-1} \psi_c^{(n-m)}(\mathbf{k}_1) \psi_d^{(m)}(\mathbf{k}_2), \quad (19)$$

where

$$\sigma_{ab}(n) = \frac{1}{(2n+3)(n-1)} \begin{bmatrix} 2n+1 & 2 \\ 3 & 2n \end{bmatrix}. \quad (20)$$

Equation (19) is the equivalent to the Goroff et al. (1986) recursion relations, Eqs. (10-11), for the n^{th} order Fourier amplitude solutions $\psi_a^{(n)}(\mathbf{k})$. It turns out

to be convenient to write down the equation of motion Eq. (13) in integral form. Laplace transformation in the variable z leads to:

$$\sigma_{ab}^{-1}(\omega) \Psi_b(\mathbf{k}, \omega) = \phi_a(\mathbf{k}) + \gamma_{abc}(\mathbf{k}, \mathbf{k}_1, \mathbf{k}_2) \oint \frac{d\omega_1}{2\pi i} \Psi_b(\mathbf{k}_1, \omega_1) \Psi_c(\mathbf{k}_2, \omega - \omega_1), \quad (21)$$

where $\phi_a(\mathbf{k})$ denote the initial conditions, that is $\Psi_a(\mathbf{k}, z = 0) \equiv \phi_a(\mathbf{k})$. Multiplying by the matrix σ_{ab} , and performing the inversion of the Laplace transform we finally get

$$\Psi_a(\mathbf{k}, z) = g_{ab}(z) \phi_b(\mathbf{k}) + \int_0^z dz' g_{ab}(z - z') \gamma_{bcd}(\mathbf{k}, \mathbf{k}_1, \mathbf{k}_2) \Psi_c(\mathbf{k}_1, z') \Psi_d(\mathbf{k}_2, z'), \quad (22)$$

where the *linear propagator* $g_{ab}(z)$ is defined as ($c > 1$ to pick out the standard retarded propagator, Scoccimarro 1998)

$$g_{ab}(z) = \oint_{c-i\infty}^{c+i\infty} \frac{d\omega}{2\pi i} \sigma_{ab}(\omega) e^{\omega z} = \frac{e^z}{5} \begin{bmatrix} 3 & 2 \\ 3 & 2 \end{bmatrix} - \frac{e^{-3z/2}}{5} \begin{bmatrix} -2 & 2 \\ 3 & -3 \end{bmatrix}, \quad (23)$$

for $z \geq 0$, whereas $g_{ab}(z) = 0$ for $z < 0$ due to causality, $g_{ab}(z) \rightarrow \delta_{ab}$ as $z \rightarrow 0^+$. The first term in Eq. (23) represents the propagation of linear growing mode solutions, where the second corresponds to the decaying modes propagation. If we assume that the initial conditions are set in the growing mode, then $\phi_a(\mathbf{k}) = \delta_1(\mathbf{k})(1, 1)$ and the second term in Eq. (23) does not contribute upon contraction with $\phi_b(\mathbf{k})$. Consistently with this, we can neglect subdominant time dependences in the non-linear term in Eq. (22), which amounts to setting the initial conditions at $z = -\infty$. Then, the equations of motion in integral form reduce to:

$$\Psi_a(\mathbf{k}, z) = e^z \phi_a(\mathbf{k}) + \int_{-\infty}^z dz' g_{ab}(z - z') \gamma_{bcd}(\mathbf{k}, \mathbf{k}_1, \mathbf{k}_2) \Psi_c(\mathbf{k}_1, z') \Psi_d(\mathbf{k}_2, z'). \quad (24)$$

As it stands, this integral equation can be thought as an equation for $\Psi_a(\mathbf{k}, z)$ in the presence of an “external source” $\phi_a(\mathbf{k})$ with prescribed statistics. In particular, if we assume that the initial conditions are Gaussian; then the statistical properties of $\phi_a(\mathbf{k})$ are completely characterized by its two-point correlator

$$\langle \phi_a(\mathbf{k}) \phi_b(\mathbf{k}') \rangle = \delta_D(\mathbf{k} + \mathbf{k}') u_{ab} P(k), \quad (25)$$

where $P(k)$ denotes the initial power spectrum of density fluctuations and $u_{ab} = 1$ for growing-mode initial conditions. From Eq. (24), it is easy to verify that the ansatz in Eq. (17) leads to the recursion relations in Eq. (19).

Equation (22) has a simple interpretation. The first term corresponds to the linear propagation from the initial conditions, whereas the second term contains information on non-linear interactions (mode-mode coupling). This corresponds to all the interactions between waves that happen at time z' (with $0 \leq z' \leq z$)

characterized by γ_{bcd} and then propagated forward in time from z' to z by the propagator $g_{ab}(z - z')$. We can also write down the general solution as a perturbation series,

$$\psi_a^{(n)}(\mathbf{k}, z) = \int \delta_D(\mathbf{k} - \mathbf{k}_{1\dots n}) \mathcal{F}_a^{(n)}(\mathbf{k}_1, \dots, \mathbf{k}_n; z) \delta_1(\mathbf{k}_1) \dots \delta_1(\mathbf{k}_n), \quad (26)$$

where the kernels satisfy the usual recursion relations

$$\mathcal{F}_a^{(n)}(z) = \sum_{m=1}^n \int_0^z ds g_{ab}(z - s) \gamma_{bcd}(\mathbf{k}, \mathbf{k}_1, \mathbf{k}_2) \mathcal{F}_c^{(m)}(s) \mathcal{F}_d^{(n-m)}(s). \quad (27)$$

Interactions modify the linear propagator, leading to *propagator renormalization*, so that the non-linear propagator defined by

$$G_{ab}(k, z) \delta_D(\mathbf{k} - \mathbf{k}') \equiv \left\langle \frac{\delta \Psi_a(\mathbf{k}, z)}{\delta \phi_b(\mathbf{k}')} \right\rangle_c, \quad (28)$$

reads

$$G_{ab}(k, z) = g_{ab}(z) + \sum_{n=1}^{\infty} A_n(z) \int d^3 q_1 P_1 \dots d^3 q_n P_n \frac{\partial \overline{\mathcal{F}}_a^{(2n+1)}}{\partial u_b}, \quad (29)$$

where $\overline{\mathcal{F}}_a^{(2n+1)} = \mathcal{F}_a^{(2n+1)}(\mathbf{k}, \mathbf{q}_1, -\mathbf{q}_1, \dots, \mathbf{q}_n, -\mathbf{q}_n)$, $A_n(z) \equiv (2n - 1)!! \exp[(2n + 1)z]$, and we defined $\phi_b \equiv (u_1, u_2) \delta_1(\mathbf{k})$. Similarly the vertex is renormalized by non-linear interactions as well,

$$\Gamma_{abc}(\mathbf{k}_1, \mathbf{k}_2, z) \delta_D(\mathbf{k} - \mathbf{k}_{12}) \equiv G_{bd}^{-1} G_{ce}^{-1} \left\langle \frac{\delta^2 \Psi_a(\mathbf{k}, z)}{\delta \phi_d(\mathbf{k}_1) \delta \phi_e(\mathbf{k}_2)} \right\rangle_c, \quad (30)$$

and thus $\Gamma_{abc} = \gamma_{abc} + \text{corrections}$.

The calculation of correlation functions can be written down in terms of Feynman diagrams (Figs. 1-2). We assign a solid line to each propagator, Eq. (23), a crossed circle represents the two-point correlator in the initial conditions, Eq. (25), and a solid circle represent the vertex, Eqs. (15-16). In this representation, loop corrections can be divided into two general classes, those which renormalize the propagator, and those which renormalize the vertex. For example, in the calculation of the one-loop power spectrum there are two contributions, $P^{(1)} = \langle \delta_1 \delta_3 + \delta_2 \delta_2 \rangle_c$ (where δ_i denotes the i^{th} order solution in PT); the $\langle \delta_1 \delta_3 \rangle_c$ term corresponds to renormalizing the propagator (first one-loop term in Fig. 1), whereas the $\langle \delta_2 \delta_2 \rangle_c$ term denotes the irreducible one-loop power spectrum (second one-loop term in Fig. 1). By irreducible, we mean that this contribution cannot be separated into two connected diagrams by cutting one internal propagator line, unlike the $\langle \delta_1 \delta_3 \rangle_c$ contribution.

For the bispectrum, the 4 one-loop terms can be divided in a similar fashion. The $\langle \delta_4 \delta_1^2 \rangle_c$ corresponds to vertex renormalization (first one-loop term in Fig. 2), the $\langle \delta_3 \delta_2 \delta_1 \rangle_c$ correspond to power spectrum (second one-loop term in Fig. 2) and

propagator renormalization (third one-loop term in Fig. 2), and the $\langle \delta_2^3 \rangle_c$ gives the irreducible one-loop bispectrum (last term in Fig. 2). This formalism can also be extended to include non-Gaussian initial conditions, see Scoccimarro (1998) for a general discussion and the specific example of Zel'dovich approximation initial conditions, relevant to transients in N-body simulations.

3. One-Loop Propagator and The Non-Linear Power Spectrum

As an example, we calculate the one-loop propagator, $G_{ab}^{(1)}$

$$G_{ab}^{(1)}(k, z) = g_{ab}(z) + \exp(3z) \int d^3q P(q) \frac{\partial \mathcal{F}_a^{(3)}}{\partial u_b}(\mathbf{k}, \mathbf{q}, -\mathbf{q}; z), \quad (31)$$

If we take the $k \rightarrow 0$ limit, we find that (keeping only the fastest growing term)

$$G_{ab}^{(1)}(k, z) = g_{ab}(z) - \sigma_v^2 \exp(3z) \begin{bmatrix} 9/50 & 61/1050 \\ 3/25 & 61/1575 \end{bmatrix}, \quad (32)$$

where $\sigma_v^2 \equiv \int P(q) d^3q/q^2$. Since the correction is negative, this tends to make the non-linear growth smaller than in linear theory, particularly for linearly decaying modes, which decay faster than in the linear case. The correction to g_{ab} can be rewritten in terms of a correction to Ω_{ab} , using that

$$(\partial_z G_{ab}) G_{bc}^{-1} = -\Omega_{ac}, \quad (33)$$

so that

$$\delta\Omega_{ab} \approx k^2 \sigma_v^2 \exp(7z/2) \begin{bmatrix} -28/375 & 28/375 \\ -4/75 & 4/75 \end{bmatrix}. \quad (34)$$

In order to see the role of decaying modes in the standard solutions of non-linear PT, let's consider the usual second-order PT kernel (e.g. relevant for the calculation of the skewness and bispectrum). In our notation, the second-order kernel can be written as

$$\mathcal{F}_1^{(2)}(\mathbf{k}_1, \mathbf{k}_2) = \int_0^z ds g_{1b}(z-s) \gamma_{bcd} \exp(2s) (1, 1)_c (1, 1)_d, \quad (35)$$

where we assumed linear growing mode initial conditions. Since $g_{1b}\gamma_{bcd} = g_{11}\gamma_{121} + g_{12}\gamma_{222}$, and using Eq. (23) we have for the fastest growing contribution to 2nd-order PT

$$\begin{aligned} \mathcal{F}_1^{(2)}(\mathbf{k}_1, \mathbf{k}_2) &= \exp(2z) \left[\left(\frac{3}{5} + \frac{4}{35} \right) \alpha(\mathbf{k}, \mathbf{k}_1) + \left(\frac{2}{5} - \frac{4}{35} \right) \beta(\mathbf{k}_1, \mathbf{k}_2) \right] \\ &= \exp(2z) \left[\frac{5}{7} \alpha(\mathbf{k}, \mathbf{k}_1) + \frac{2}{7} \beta(\mathbf{k}_1, \mathbf{k}_2) \right]. \end{aligned} \quad (36)$$

It is crucial to note here that the $4/35$ contributions come from *linearly decaying* modes; that is, after scattering, waves are not in linearly growing modes anymore, and this type of amplitude propagated into the present time contributes $4/35$ to the amplitudes of second-order PT kernels. That means that if we are using the kernels to calculate one-loop corrections, which are important at intermediate k 's, one could use the approximation in Eq. (34) to improve the propagator in Eq. (35); in this case this corresponds to suppressing the linearly decaying mode contribution to the propagator. As a result, the 2nd-order PT kernel at intermediate scales would look more like

$$\mathcal{F}_1^{(2)}(\mathbf{k}_1, \mathbf{k}_2) = \exp(2z) \left[\frac{3}{5} \alpha(\mathbf{k}, \mathbf{k}_1) + \frac{2}{5} \beta(\mathbf{k}_1, \mathbf{k}_2) \right]. \quad (37)$$

This means that a simple way of improving one-loop corrections in PT, is to use the kernels obtained by ignoring the linearly decaying modes contributions. This has the effect of incorporating higher-order loop corrections (those corresponding to propagator renormalization, although only approximately since we don't use the full one-loop propagator) in the usual formulation of PT.

If we suppress linearly decaying mode contributions for the third-order kernel and use this to calculate one-loop corrections to the power spectrum, we find the results in Figs.3-4. The solid lines in Fig. 3 show the standard (top) and “improved” (bottom) calculations of the non-linear power spectrum, whereas the dashed line shows the fitting formula for the non-linear power spectrum. The three-remaining solid lines (which extend up to $k \approx 3$ h/Mpc) denote the measurement in N-body simulations of the density power spectrum, the velocity divergence power spectrum and the velocity vorticity power spectrum, as labeled. We see that the vorticity power spectrum is certainly negligible at large scales, and it does not become significant until scales of order $k \approx 2$ h/Mpc. At small scales, we find that the vorticity spectrum is roughly twice that of the divergence, as expected if the velocity field has equal power in all directions relative to \mathbf{k} .

Note that the “improved” calculation is somewhat smaller than the standard one-loop calculation, as expected since the contribution from propagating linearly decaying modes has been suppressed. Overall the agreement with the N-body results is better. In Fig. 4 we show the ratio of our predictions for different models to the non-linear fitting formula, the horizontal dashed lines show the expected accuracy of the latter. We see that the “improved” calculations (solid) stay within the non-linear fitting formula accuracy up to $k \approx 5$ h/Mpc, whereas the standard one-loop calculation (dashed) overestimates the non-linear power spectrum at scales smaller than the non-linear scale, $k \approx 0.3$ h/Mpc. The improvement is thus quite significant, although we have included the effects of propagator renormalization in a crude way.

Unlike the velocity divergence, which can be calculated in one-loop PT in analogous fashion to the density power spectrum, understanding the vorticity power spectrum is considerably more complicated because vorticity is generated by shell-crossing, an effect which is neglected in the formulation of PT (see e.g. Pichon & Bernardeau, 1999). However, we can understand approximately the scaling with redshift and scale from simple considerations. After shell-crossing, vorticity develops because what we see is the mass average of different streams, each with its own (irrotational) velocity field. Thus, vorticity can be thought as coming from the vorticity of the mass-weighted velocity field, i.e.

$$\mathbf{w} \sim f_v(\tau) \nabla \times [(1 + \delta)\mathbf{v}], \quad (38)$$

where $f_v(\tau)$ is the fraction of volume that undergoes shell-crossing at time τ . We can then write the vorticity power spectrum ($\langle \mathbf{w}(\mathbf{k}) \cdot \mathbf{w}(\mathbf{k}') \rangle \equiv P_w(k)\delta_D(\mathbf{k} + \mathbf{k}')$)

$$P_w(k) \sim f_v^2(\tau) \int \frac{|\mathbf{k} \times \mathbf{q}|}{q^4} [P_\theta(|\mathbf{k} - \mathbf{q}|)P_\delta(q) - P_x(|\mathbf{k} - \mathbf{q}|)P_x(q)] d^3q, \quad (39)$$

where $P_\theta(k)$ is the velocity divergence power spectrum and $P_x(k)$ is the power spectrum of the density-velocity divergence cross-correlation. The simplest approximation would be to use linear PT (although it is unlikely to be valid for each flow at the scales of interest); however, since $P_\theta = P_\delta = P_x$ in linear PT, this contribution vanishes. Thus, the leading-order contribution to $P_w(k)$ comes from one-loop PT,

$$P_w(k) \sim f_v^2(\tau) k^2 \int \frac{d^3q}{q^2} a^6 |k - q|^{2n+3} q^n \sim a^6 f_v^2 k^{3n+6}. \quad (40)$$

Thus, we expect a strong time and scale dependence for the vorticity power spectrum. The latter is in reasonable agreement with Fig. 3, the time dependence is more difficult to test due to the unknown dependence coming from $f_v^2(\tau)$.

4. Conclusions

We described a new approach to gravitational instability in large-scale structure, where the equations of motion are written and solved as in field theory in terms of Feynman diagrams. The basic objects of interest are the propagator (which propagates solutions forward in time), the vertex (which describes non-linear interactions between waves) and a source with prescribed statistics which describes the effect of initial conditions. Loop corrections renormalize these quantities, in particular, decaying modes are suppressed in the one-loop propagator compared to linear PT. We used this to construct the PT kernels and calculate “improved” loop corrections, these include effects beyond standard one-loop PT calculations, leading to better agreement with N-body simulations for the evolution of the power spectrum. We also consider the role of vorticity creation due to shell-crossing and show using N-body simulations that at small (virialized) scales the velocity field reaches equipartition, i.e. the vorticity power spectrum is about twice the divergence power spectrum. We also sketched a derivation of the time dependence and scaling of the vorticity power spectrum.

Our calculations are only a first attempt to include the effects of propagator renormalization, more work is needed to confirm that the results presented here are indeed robust to a more careful treatment. We have also neglected vertex renormalization. On the other hand, it seems that this approach can lead to useful insights into the nature of non-linear corrections and perhaps give us a more accurate way to calculate clustering statistics in the transition to the non-linear regime. Our results on the vorticity from numerical simulations suggest that there is a significant range of scales until the assumption of irrotational fluid breaks down. We hope that by using these techniques we can finally answer the question: “Why does PT work so well?”

5. Acknowledgements

I thank Francis Bernardeau and Dmitry Pogosyan for useful discussions.

References

- Bernardeau, F., 1992, *The Gravity-Induced Quasi-Gaussian Correlation Hierarchy*, ApJ **392**: 1-14.
- Bernardeau, F., 1994, *The Effects of Smoothing on the Statistical Properties of Large-Scale Cosmic Fields*, A&A **291**: 697-712.
- Fosalba, P. & E. Gaztañaga, 1998, *Cosmological Perturbation Theory and the Spherical Collapse Model - I. Gaussian Initial Conditions*, MNRAS **301**: 503-523.
- Fry, J.N., 1984, *The Galaxy Correlation Hierarchy in Perturbation Theory*, ApJ**279**: 499-510.
- Gaztañaga, E. & P. Fosalba, 1998, *Cosmological Perturbation Theory and the Spherical Collapse Model - II. Non-Gaussian Initial Conditions*, MNRAS **301**: 524-534.
- Goroff, M. H., B. Grinstein, S.-J. Rey & M. B. Wise, 1986, *Coupling of Modes of Cosmological Mass Density Fluctuations*, ApJ **311**: 6-14.
- Pichon, C. & F. Bernardeau, 1999, A&A **343**, 663-681
- Scoccimarro, R. & J.A. Frieman, 1996, *Loop Corrections in Non-Linear Cosmological Perturbation Theory*, ApJS **105**, 37-73
- Scoccimarro, R., 1997, *Cosmological Perturbations: Entering the Non-Linear Regime*, ApJ **487**, 1-17
- Scoccimarro, R., S. Colombi, J.N. Fry, J.A. Frieman, E. Hivon & A. Melott, 1998, *Non-Linear Evolution of the Bispectrum of Cosmological Perturbations*, ApJ **496**, 586-604.
- Scoccimarro, R., 1998, *Transients from Initial Conditions: A Perturbative Analysis*, MNRAS **299**: 1097-1118.

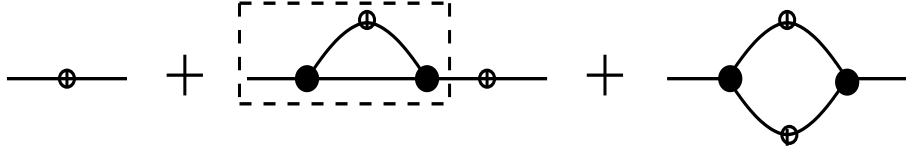


Figure 1. Power spectrum diagrams up to one-loop. The first term denotes the linear contribution, the two remaining terms denote the one-loop correction. The factor enclosed by dashed lines denotes propagator renormalization.

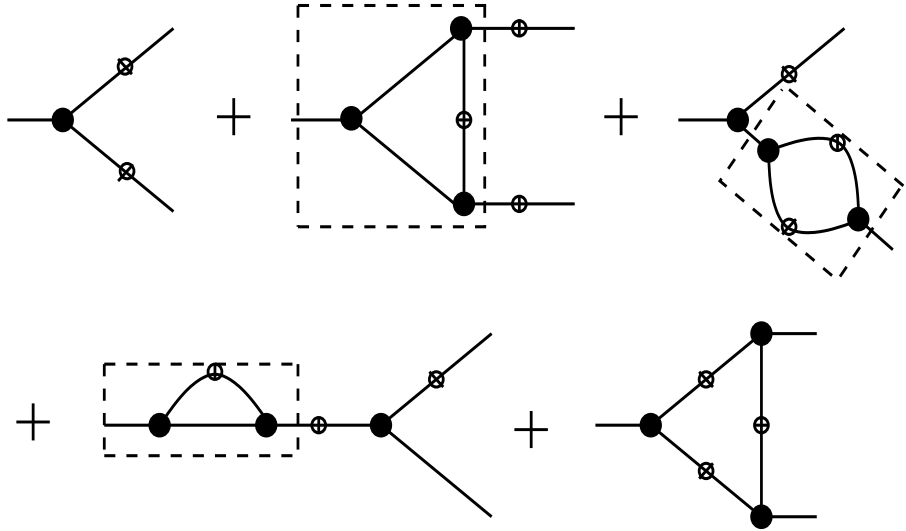


Figure 2. Bispectrum diagrams up to one-loop. The first terms denotes the tree contribution, the four remaining terms the one-loop correction. The first factor enclosed by dashed lines denotes vertex renormalization, the second corresponds to the irreducible one-loop power spectrum, the third denotes propagator renormalization. The last term gives the irreducible one-loop bispectrum.

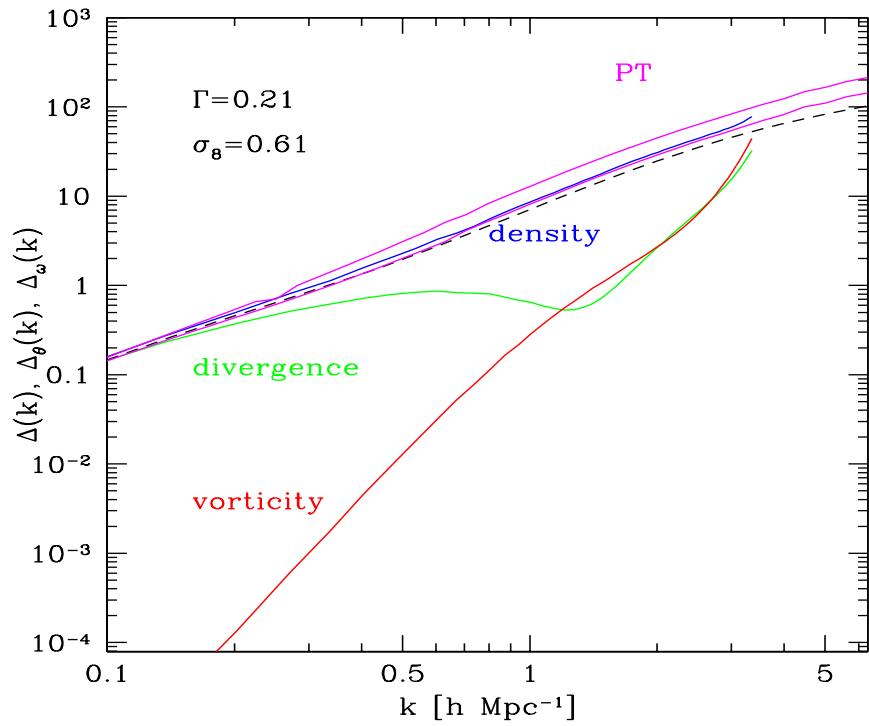


Figure 3. The power spectrum of the density, velocity divergence and vorticity as a function of scale. The two solid lines roughly parallel at high- k are the standard one-loop PT density power spectrum calculation (top) and the new one-loop approach (bottom). The dashed line denotes the prediction of the fitting formula and the solid line close to it the actual measurement in the N-body simulation. The two other solid lines denote the power spectrum of the velocity divergence and vorticity, as labeled.

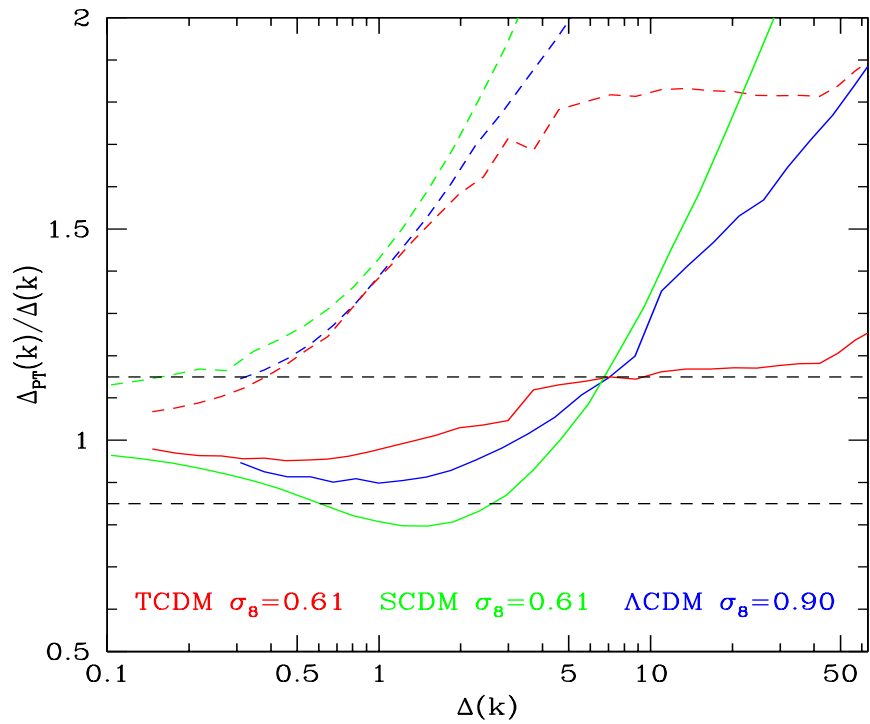


Figure 4. Ratio of predictions from one-loop PT (standard in dashed lines, new approach in solid lines) to the fitting formula for the non-linear power spectrum. The three different curves are for three different models, as labeled.